BUTTERWORTH HEINEMANN

Polymer Vol. 36 No. 9, pp. 1893–1902, 1995

0032-3861/95/$10.00 + 0.00

Liquid crystalline polyimides: 18. Thermotropic polyimides based on biphenyl-3,3′,4,4′-tetracarboxylic anhydride

Hans R. Kricheldorf* and Volker Linzer
Institut für Technische und Makromolekulare Chemie, Bundesstrasse 45, D-20146 Hamburg, Germany
(Received 13 May 1994)

Polyimides were prepared from α,ω-bis(4-aminophenoxy)alkanes and various aromatic tetracarboxylic anhydrides. Only the polyimides derived from biphenyl-3,3′,4,4′-tetracarboxylic anhydride form a liquid crystalline (LC) melt. In contrast, polyimides of the same dianhydride and α,ω-diamino alkanes are crystalline but not thermotropic. The mesogenic and non-mesogenic behaviour of the various poly(ester–imide)s is discussed on the basis of conformational differences calculated by a force-field program. The polyimides were characterized by elemental analyses, viscosity measurements, infra-red and nuclear magnetic resonance spectroscopies and differential scanning calorimetry measurements at variable temperatures. The formation of 'batonet' and 'fan-shaped' textures along with the wide-angle X-ray diffraction patterns suggest that the LC polyimides form a smectic A phase in addition to a smectic crystalline phase. Both melting and isotropization temperatures show an odd–even effect.

(Keywords: polyimides; liquid crystallinity; mesogen conformation)

INTRODUCTION

Aromatic imide groups such as pyromellitic imide or derivatives of phthalimide are almost planar, rigid, polar and thermostable, and thus should be favourable components of liquid crystalline (LC) polymers regardless of whether thermotropic or lyotropic character is taken into consideration. However, the huge amount of work invested by numerous research groups into the synthesis and characterization of a broad variety of polyimides over the past four decades has revealed that LC polyimides are difficult to find[1–8]. The best chance to obtain a thermotropic polyimide consists of a combination of ester and imide groups in a polymer chain[9–20], the ester groups imparting flexibility and linearity into the overall conformation. To the best of our knowledge, thermotropic polyimides free of ester groups have never been reported before. The present work describes for the first time thermotropic smectic polyimides devoid of ester groups.

EXPERIMENTAL

Materials

Benzophenone-3,3′,4,4′-tetracarboxylic anhydride, diphenylether-3,3′,4,4′-tetracarboxylic anhydride, diphenylsulfone-3,3′,4,4′-tetracarboxylic anhydride and biphenyl-3,3′,4,4′-tetracarboxylic anhydride were purchased from Kennedy and Kim (Little Silver, NJ, USA). They were recrystallized from dioxane and acetic anhydride. 1,9-Diaminonane, 1,10-diaminodecane, 1,7-dibromoheptane, 1,8-dibromooctane, 1,9-dibromononane, 1,10-dibromodecane, 1,11-dibromoundecane and 1,12-dibromododecane were purchased from Aldrich Co. (Milwaukee, WI, USA). *m*-Cresol and 4-nitrophenol were gifts from Bayer Co. (Leverkusen, Germany).

α,ω-Bis(4-nitrophenoxy)alkanes (Table 1)

Trimethylsilyl 4-nitrophenol (0.5 mol) and dry K_2CO_3 (0.25 mol) (finely powdered) were added to dry dimethylformamide (100 ml). A solution of an α,ω-dibromoalkane (0.24 mol) in dry dimethylformamide (50 ml) was added dropwise with stirring. After complete addition the reaction mixture was heated for 6 h at 120°C, cooled and poured onto crushed ice. The precipitated yellow product was isolated by filtration, dissolved in CH_2Cl_2 and washed successively with 2 M NaOH, 1 M HCl and water. The CH_2Cl_2 solution was then dried over Na_2SO_4 and concentrated *in vacuo*, and the product crystallized by portion-wise addition of ligroin. This crude product was recrystallized from ethanol.

α,ω-Bis(4-aminophenoxy)alkanes (Table 2)

An α,ω-bis(4-nitrophenoxy)alkane (0.1 mol) was dissolved in tetrahydrofuran (1 l), Pt on charcoal (10%) was added (5 g) and the reaction mixture was purged with nitrogen. The nitrogen was then replaced by a hydrogen atmosphere and the hydrogenation was completed within 36 h by shaking of the reaction mixture. After renewed purging with nitrogen, the catalyst was filtered off, the filtrate was concentrated *in vacuo* and the product crystallized by portion-wise addition of ligroin. The crude product was recrystallized from hot tetrahydrofuran

* To whom correspondence should be addressed

containing 10–20 mol% of water depending on the solubility.

Polycondensations (Tables 3 and 4)

A diamine (15 mmol) and a freshly recrystallized dianhydride were dissolved in *m*-cresol (250 ml). This reaction mixture was stirred under nitrogen for 2 h at 180°C. The temperature was then raised by 15–20°C and the liberated water was slowly distilled off. The lost *m*-cresol was permanently replaced from a dropping funnel (duration ~2 h). After cooling to ~60°C, the reaction mixture was poured into hot ethanol. The precipitated polymer was filtered off, extracted with hot ethanol and dried at 120°C *in vacuo*.

Measurements

The inherent viscosities (η_{inh}) were measured with an automated Ubbelohde viscometer thermostated at 25°C. The measurements were performed at a concentration, *c*, of 2 g l^{-1} in CH_2Cl_2/trifluoracetic acid (9:1 v/v).

Infra-red (i.r.) spectra were recorded with a Nicolet SXB-20 FT spectrometer from KBr pellets.

^{1}H nuclear magnetic resonance (n.m.r.) spectra were obtained on a Bruker AC-100 FT spectrometer in 5 mm o.d. sample tubes. $CDCl_3$ containing 20 vol% of trifluoroacetic acid and tetramethylsilane (TMS) for shift referencing served as solvent.

Differential scanning calorimetry (d.s.c.) measurements were conducted with a Perkin–Elmer DSC-4 at a heating and cooling rate of 20°C min^{-1} in aluminium pans under nitrogen.

Wide-angle X-ray diffraction (WAXD) powder patterns were recorded at room temperature with a Siemens D-500 diffractometer using Ni-filtered Cu Kα radiation. Temperature-dependent measurements were conducted with synchrotron radiation at HASYLAB (DESY) Hamburg, Germany. A wavelength of 1.50 Å, a position-sensitive one-dimensional detector and a heating rate of 20°C min^{-1} were used.

RESULTS AND DISCUSSION

Syntheses

All polyimides studied in this work were prepared by direct polycondensation of diamines with aromatic tetracarboxylic dianhydrides. Whereas the anhydrides are commercial products, the diamines **2a–f**, **4a**, **5a** and **6a** (*Scheme 1*) had to be synthesized. Their synthesis was conducted in a two-step procedure. First, silylated 4-nitrophenol was alkylated with α,ω-dibromoalkane to give the α,ω-bis-4(nitrophenoxy)alkanes.

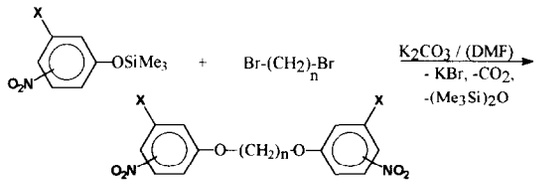

This procedure gave considerably higher yields than the alkylation of free nitrophenols. The bis(nitrophenoxy)-alkanes **3a–f**, **4b**, **5b** and **6b** (*Scheme 1*) were then hydrogenated by means of a Pt catalyst to give the corresponding diamines. In this connection, it should be noted that the synthesis of some of the diamine spacers has already been reported in the literature[21]. The yields and properties of all nitro compounds are compiled in *Table 1*, and those of the spacer diamines are given in *Table 2*. The chemical structures of all diamines and their precursors were checked by ^{1}H n.m.r. spectroscopy as illustrated in *Figure 1*.

All polycondensations of diamines with dianhydrides were conducted in boiling *m*-cresol with azeotropic removal of water. Three classes of polyimides were

Table 1 Yields and properties of α,ω-bis(4-nitrophenoxy)alkanes

Compound	*n*	Yield (%)	M.p. (°C)	Elemental formula (molecular wt) (g mol^{-1})	Elemental analysis (%)			
						C	H	N
3a	7	86	117–118	$C_{19}H_{22}N_2O_6$	Calc.	60.95	5.92	7.48
				(374.4)	Found	60.65	5.96	7.30
3b	8	62	119–120	$C_{20}H_{24}N_2O_6$	Calc.	61.85	6.23	7.21
				(388.4)	Found	60.77	6.44	7.19
3c	9	80	89–90	$C_{21}H_{26}N_2O_6$	Calc.	62.67	6.51	6.96
				(402.4)	Found	61.92	6.80	6.77
3d	10	78	81–82	$C_{22}H_{28}N_2O_6$	Calc.	63.45	6.78	6.73
				(416.5)	Found	62.88	6.93	6.52
3e	11	86	76–78	$C_{23}H_{30}N_2O_6$	Calc.	64.17	7.02	6.51
				(430.5)	Found	63.03	7.09	6.33
3f	12	80	77–78	$C_{24}H_{32}N_2O_6$	Calc.	64.85	7.26	6.30
				(444.5)	Found	64.12	7.40	6.29
4b	10	79	79–80	$C_{22}H_{28}N_2O_6$	Calc.	63.45	6.78	6.73
				(416.5)	Found	63.01	6.99	6.51
5b	10	87	69–70	$C_{22}H_{28}N_2O_6$	Calc.	63.45	6.78	6.73
				(416.5)	Found	62.29	6.89	6.58
6b	10	88	89–91	$C_{24}H_{32}N_2O_6$	Calc.	64.85	7.26	6.30
				(444.5)	Found	63.87	7.84	6.05

prepared: **7a**, **b**, **8a–f**, **9a**,**b**, **10** and **11a–c** (*Scheme 2*). The yields and properties of polyimides **7a**,**b**, **9a**,**b**, **10** and **11a–c** are compiled in *Table 3* while those of polyimides **8a–f** are summarized in *Table 4*. The i.r. spectra agree with the proposed structure because bands due to N–H vibrations are absent, whereas both CO bands typical for cyclic aromatic imide groups are present (*Figure 2*).

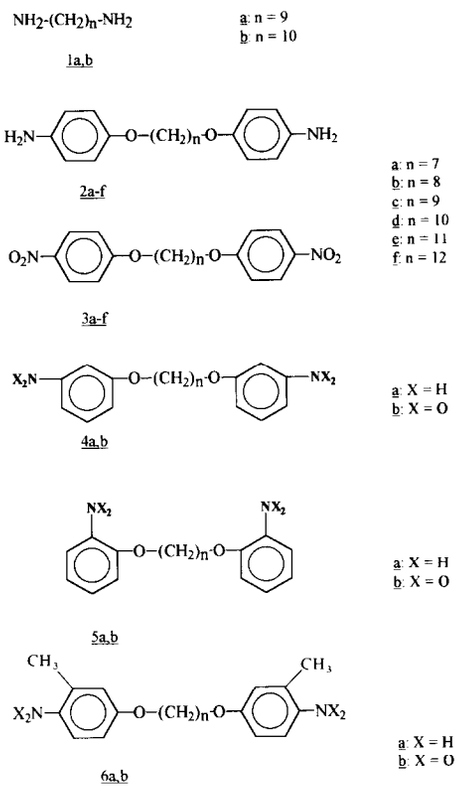

Scheme 1

The spectrum of *Figure 2* may serve as a typical example for all polyimides prepared in this work. The ^{1}H n.m.r. spectra show the expected ratio of aromatic and aliphatic protons.

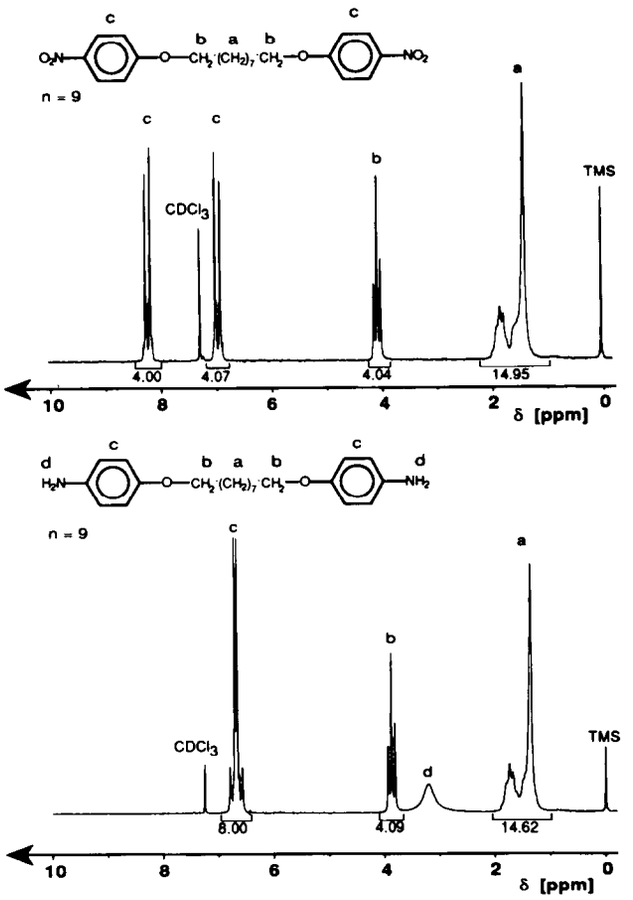

Figure 1 ^{1}H n.m.r. spectra at 100 MHz of 1,9-bis(4-nitrophenoxy)nonane (top) and 1,9-bis(4-aminophenoxy)nonane (bottom)

Table 2 Yields and properties of α,ω-bis(4-aminophenoxy)alkanes

Compound	*n*	Yield (%)	M.p. (°C)	Elemental formula (molecular wt) (g mol^{-1})	Elemental analysis (%)			
						C	H	N
2a	7	84.7	75–76	$C_{19}H_{26}N_2O_2$	Calc.	72.52	8.34	8.91
				(314.4)	Found	72.84	8.65	8.65
2b	8	73.3	130–132	$C_{20}H_{28}N_2O_2$	Calc.	73.14	8.59	8.93
				(328.5)	Found	72.78	8.67	8.39
2c	9	78.4	80–82	$C_{21}H_{30}N_2O_2$	Calc.	73.65	8.83	8.18
				(342.5)	Found	73.64	8.84	8.12
2d	10	87.5	111–112	$C_{22}H_{32}N_2O_2$	Calc.	74.12	9.05	7.86
				(356.5)	Found	73.68	8.92	7.87
2e	11	71.6	70–72	$C_{23}H_{34}N_2O_2$	Calc.	74.55	9.25	7.56
				(370.5)	Found	73.59	9.54	6.80
2f	12	90.1	111–113	$C_{24}H_{36}N_2O_2$	Calc.	74.95	9.44	7.28
				(384.6)	Found	72.35	9.44	7.02
4a	10	87.4	100–102	$C_{22}H_{32}N_2O_2$	Calc.	74.12	9.05	7.86
				(356.5)	Found	73.28	9.17	7.87
5a	10	92.6	57–58	$C_{22}H_{32}N_2O_2$	Calc.	74.12	9.05	7.86
				(356.5)	Found	72.99	9.31	7.97
6a	10	92.0	65–67	$C_{24}H_{38}N_2O_2$	Calc.	69.20	8.71	6.72
				(386.6)	Found	70.02	8.94	6.91

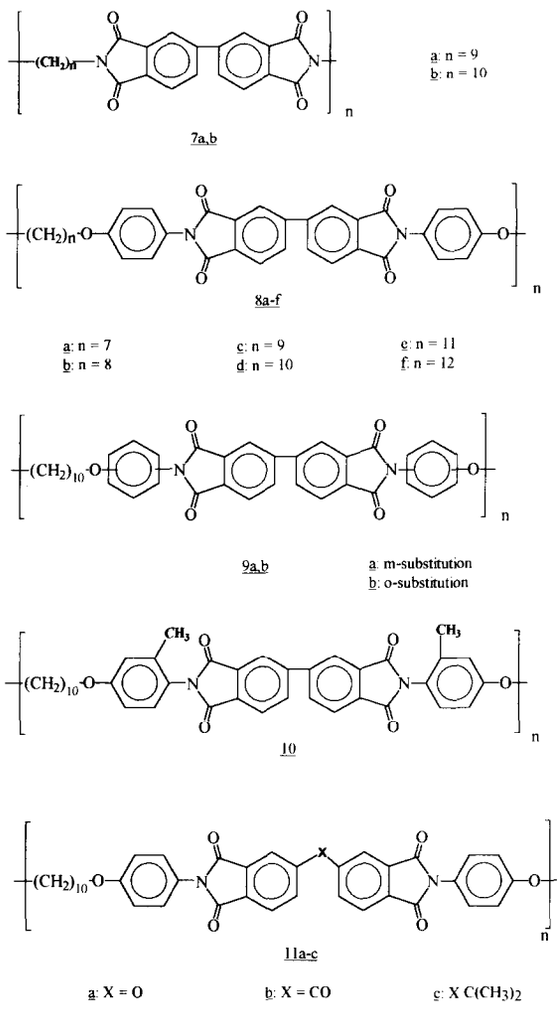

Scheme 2

Properties of polyimides 7a,b, 9a,b, 10 and 11a–c

All polyimides were characterized by optical microscopy, d.s.c. measurements and WAXD powder patterns. On the basis of this characterization, the polyimides **7a,b**, **9a,b**, **10** and **11a–c** were found to have two important properties in common: all these polyimides are semicrystalline materials and form an isotropic melt above the melting temperature (T_m in *Table 3*). The existence of short living monotropic LC phases formed upon rapid cooling was not investigated.

Nonetheless, the properties of polyimides **7a,b**, **9a,b**, **10** and **11a–c** are of interest for comparison with those of other polyimides to establish structure–property relationships of broader validity. The absence of a mobile LC phase in the case of **7a** and **b** indicates that the biphenyltetracarboxylimide unit (BTCI) is a poor mesogen. This result confirms a recent report by Sato and co-workers[22], who used this building block as a component of copolycarbonates again containing aliphatic spacers. The reason for the low mesogeneity is obviously the capability

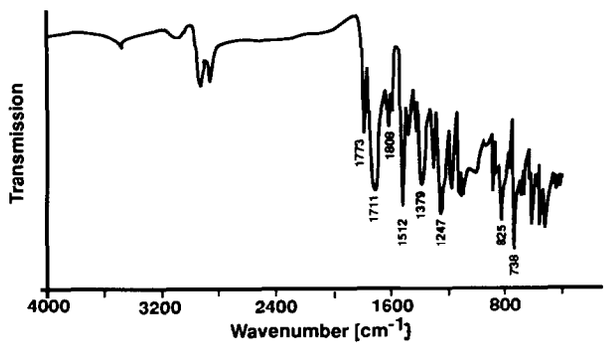

Figure 2 I.r. spectrum (KBr pellets) of the polyimide **8f**

Table 3 Yields and properties of the isotropic polyimides **7a,b**, **9a,b**, **10** and **11a–c**

Polymer	n	Yield (%)	η_{inh}[a] ($g\,dl^{-1}$)	Elemental formula (molecular wt) ($g\,mol^{-1}$)	T_g[b] (°C)	T_m[b] (°C)	Elemental analysis (%)	C	H	N
7a	9	89.5	1.15	$C_{25}H_{24}N_2O_4$ (416.48)	112	219[c]	Calc.	72.10	5.81	6.73
							Found	72.10	6.22	6.71
7b	10	92.0	0.39	$C_{26}H_{26}N_2O_4$ (430.51)	95	245	Calc.	72.54	6.09	6.51
							Found	71.79	6.13	6.70
9a	10	96.3	0.41	$C_{38}H_{34}N_2O_6$ (614.70)	123	232[c]	Calc.	74.25	5.77	4.56
							Found	73.32	5.70	4.42
9b	10	84.1	0.30	$C_{38}H_{34}N_2O_6$ (614.70)	100	-	Calc.	74.25	5.77	4.56
							Found	72.92	5.52	4.30
10	10	98.5	0.52	$C_{40}H_{38}N_2O_6$ (642.75)	153	288	Calc.	74.75	5.96	4.36
							Found	74.11	6.06	4.22
11a	10	98.1	insol.	$C_{38}H_{34}N_2O_7$ (630.70)	142	351	Calc.	72.37	5.43	4.44
							Found	71.98	5.44	4.40
11b	10	89.5	insol.	$C_{39}H_{34}N_2O_7$ (642.71)	-	396	Calc.	72.88	5.33	4.36
							Found	72.24	5.36	4.42
11c	10	95.5	0.42	$C_{41}H_{34}N_2O_6F_6$ (764.72)	153	237	Calc.	64.40	4.48	3.66
							Found	63.52	4.52	3.54

[a] Measured at 25°C with $c = 2\,g\,l^{-1}$ in CH_2Cl_2/trifluoroacetic acid (volume ratio 9:1)
[b] From d.s.c. measurements in second heating scan with a heating rate of 20°C min^{-1}
[c] Observable in the first heating curve

Table 4 Yields and properties of the thermotropic polyimides **8a–f**

Polymer	n	Yield (%)	η_{inh}[a] ($g\,dl^{-1}$)	Elemental formula (molecular wt) ($g\,mol^{-1}$)	T_g[b] (°C)	T_m[b] (°C)	T_i[b] (°C)	T_i[c] (°C)	Elemental analysis (%)	C	H	N
8a	7	93.1	insol.	$C_{35}H_{28}N_2O_6$ (572.62)	–	420	450	440–460	Calc.	73.41	4.93	4.89
									Found	72.82	4.88	4.77
8b	8	89.8	insol.	$C_{36}H_{30}N_2O_6$ (586.65)	–	426	440	430–450	Calc.	73.71	5.15	4.78
									Found	73.58	5.18	4.65
8c	9	87.1	insol.	$C_{37}H_{32}N_2O_6$ (600.67)	–	388	436	400–410	Calc.	73.98	5.37	4.66
									Found	73.53	5.44	4.58
8d	10	92.8	insol.	$C_{38}H_{34}N_2O_6$ (614.70)	–	394	430	420–430	Calc.	74.25	5.77	4.56
									Found	73.91	5.65	4.56
8e	11	84.6	insol.	$C_{39}H_{36}N_2O_6$ (628.28)	148	330	385	380–390	Calc.	74.50	5.77	4.46
									Found	73.23	5.85	3.99
8f	12	91.5	insol.	$C_{40}H_{38}N_2O_6$ (642.75)	154	374	420	420–440	Calc.	74.75	5.96	4.36
									Found	74.26	5.95	4.30

[a] Measured at 25°C with $c = 2\,g\,l^{-1}$ in CH_2Cl_2/trifluoroacetic acid (volume ratio 9:1)
[b] From d.s.c. measurements with a heating rate of $20°C\,min^{-1}$
[c] From optical microscopy with a heating rate of $10°C\,min^{-1}$

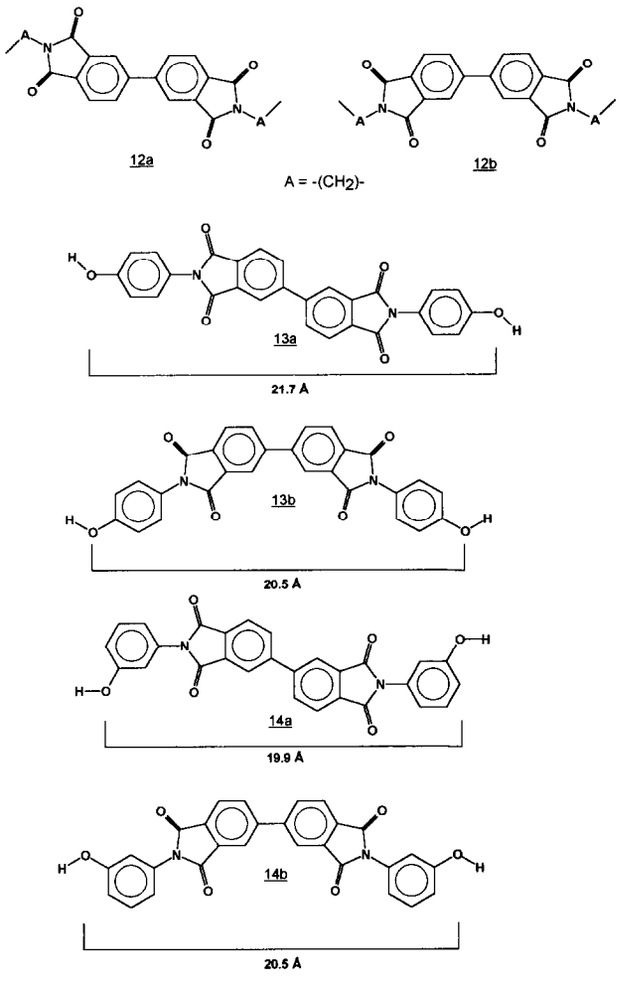

Scheme 3

of the BTCI unit to adopt a 'folded' conformation, **12b**, in addition to the 'extended' one, **12a** (*Scheme 3*). When BTCI is *N*-substituted with *p*-hydroxyphenyl groups (**13b**), a good mesogen is obtained as evidenced by the liquid crystalline character of **8a–f** (discussed below). The LC character of **8a–f** fits in with the observation that aromatic polyesters of the diphenol **13** are also thermotropic[23]. The absence of an LC phase in the case of **9a** and **b** corresponds, in turn, to the finding that polyesters derived from the diphenol **14a,b** are not thermotropic[24]. The failure of the *m*-aminophenol derivative **14** is not trivial, because the 'extended' conformation **14a** allows a linear arrangement of the ether or ester groups emanating from both ends of the diphenol. It is easier to understand that flexible and non-linear links between both 'phthalimide' groups of **11a–c** are unfavourable for the mesogenic character of the imide unit.

The most interesting result in this connection is the failure of polyimide **10** to form an LC phase. The methyl groups neither affect the linearity of the BTCI unit compared with **8d** nor significantly reduce the length/diameter ratio. However, computer modelling with the force-field program PCFF 91 (Insight II V 2.2.0/Discover V 2.8.0, from Biosym) indicates that the methyl groups hinder a coplanar conformation of phenylene and imide rings and favour a rotational angle of ~23° (*Figure 3*). The rotational barrier for the formation of the coplanar conformation is more than 100 times higher than that in the absence of methyl groups (*Figures 4* and *5*). Even if the absolute energy values calculated by the computer program are not taken too seriously, it is obvious that a coplanar conformation of polyimide **10** is considerably less favourable than in the case of **8a–f**. In this connection it should be mentioned that the most energetically favourable rotational angle of the central σ bond of the biphenyl unit amounts to 35° and the rotational barrier is as low (1–2 $kcal\,mol^{-1}$) as that of the phenyleneimide system (*Figure 4*). Therefore, the conformational properties of the biphenyl unit do not seriously hinder a nearly planar conformation of the BTCI unit.

The non-coplanar conformation of the 'mesogen' in polyimide **10** should not affect the mesogeneity, if the BTCI unit behaves as a calamitic (rod-like) mesogen as defined by Onsager[25] or Flory[26,27]. In Flory's theory, which is limited to athermal systems, the mesogeneity mainly depends on steric and entropic effects, and thus on the length/diameter ratio. However, in the preceding

part of this series[18] it was demonstrated that donor–acceptor and dipole–dipole interactions based on a coplanar array of neighbouring chain segments or mesogens may play an important role for the thermotropic character of poly(ester–imide)s. If electronic (i.e. enthalpic or thermal) interactions between the BTCI mesogens play a role, they require stacking of more or less copolanar BTCI units as illustrated in *Figure 3C*. It is obvious that the methyl substituents and the 'non-planar' conformation (*Figure 3B*) are detrimental for the postulated electronic (enthalpic) interaction, and thus for the formation of an LC phase.

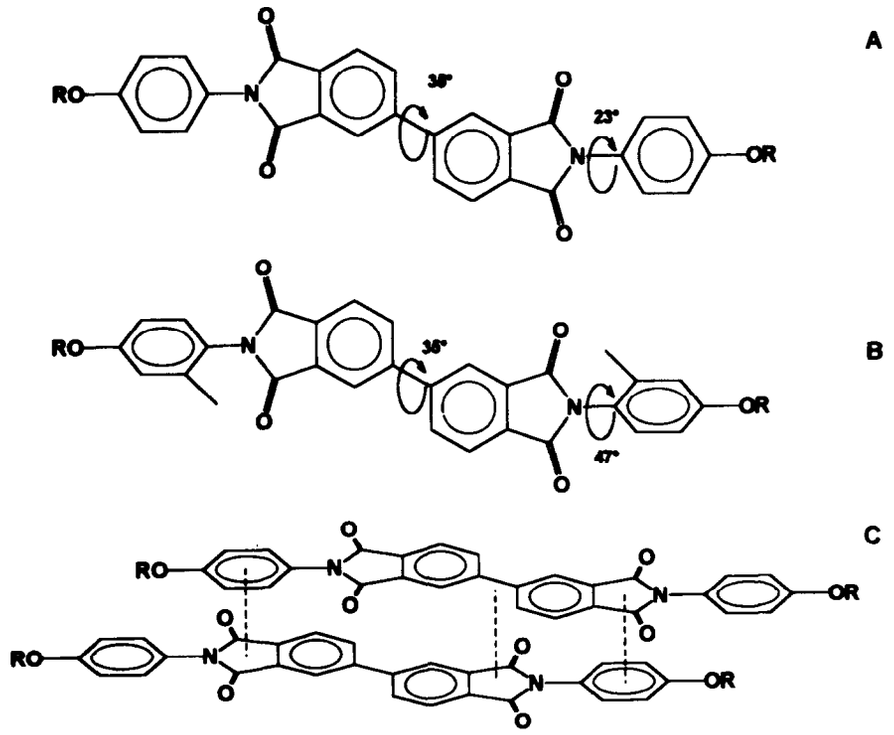

Figure 3 Schematic drawings of the most energetically favourable conformation of the mesogen in polyimides **8a–f** (A) and in polyimide **10** (B); and stacking of coplanar BTCI units favouring donor–acceptor interactions (C)

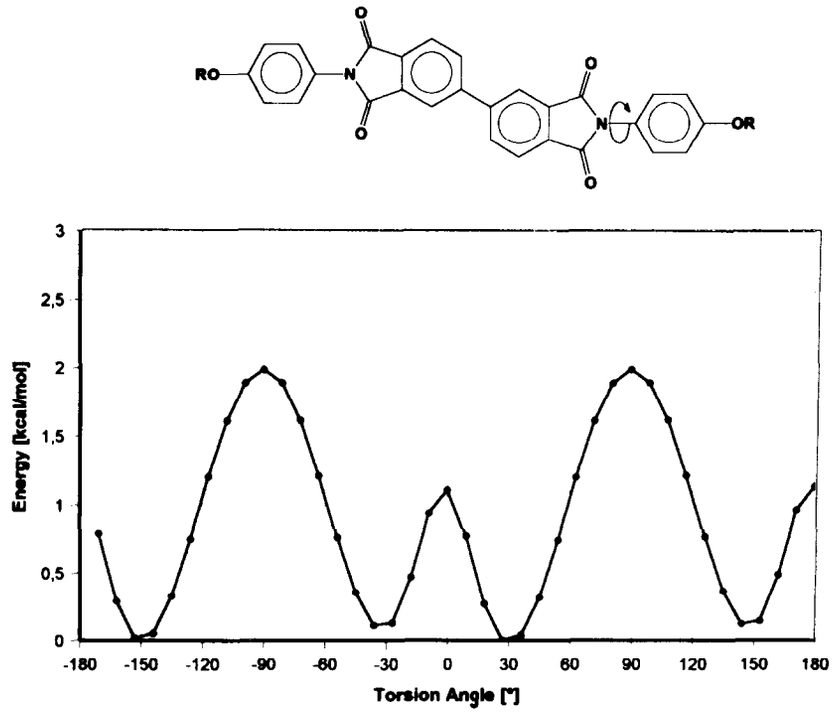

Figure 4 Energy profile for the rotation of phenylene *versus* imide ring in polyimides **8a–f** as calculated by the force-field program PCFF 91/Insight II V 2.2.0/Discover V 2.8.0 from Biosym

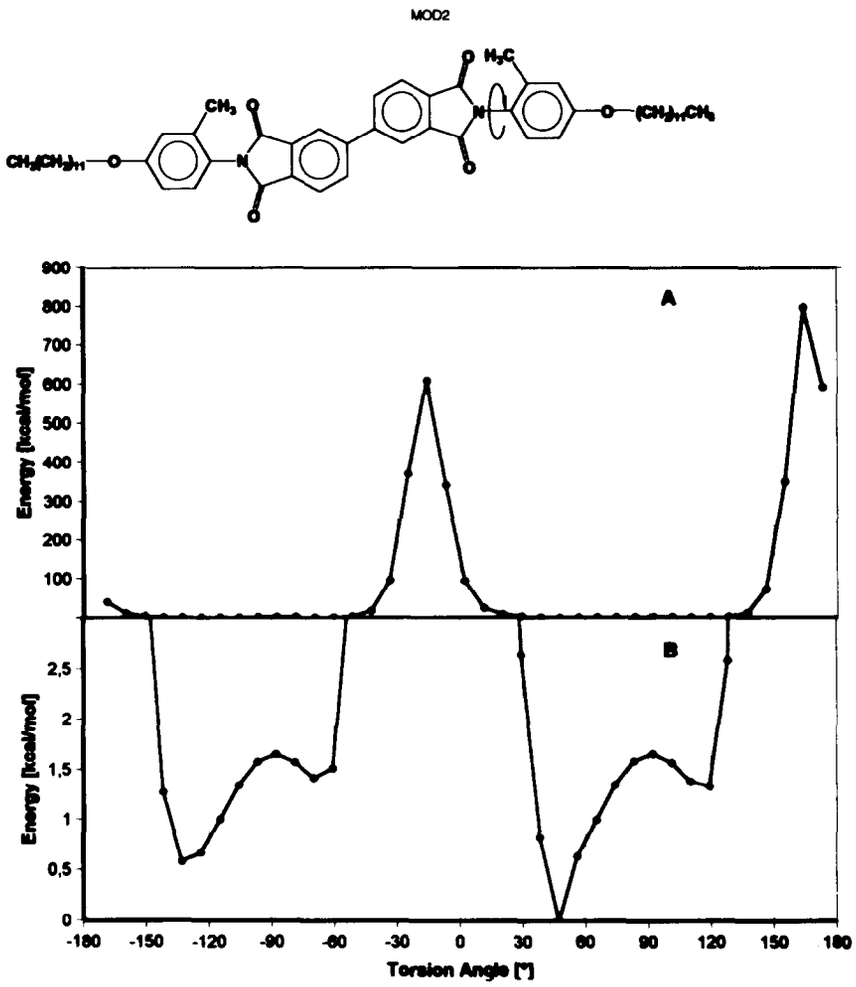

Figure 5 Energy profile for the rotation of phenylene *versus* imide ring in polyimide **10** calculated as for **8a–f** in *Figure 4*: (A) ordinate comparable with *Figure 4*; (B) ordinate showing the full height of the rotational barrier

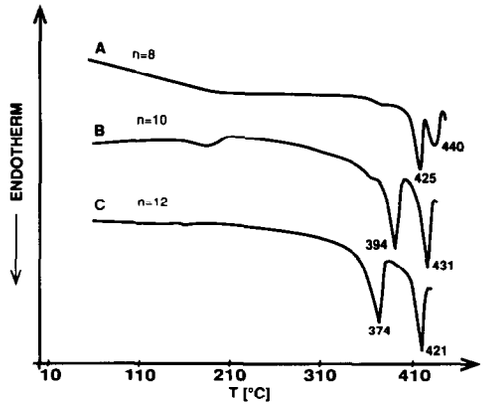

Figure 6 D.s.c. heating curves (heating rate 20°C min^{-1}) of the polyimides **8b** (A), **8d** (B) and **8f** (C)

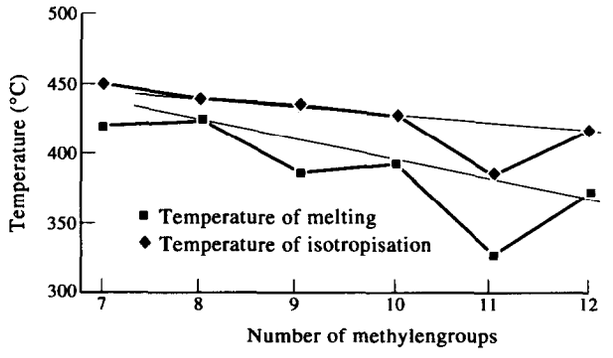

Figure 7 Plot of melting temperatures (T_m) and isotropization temperatures (T_i) *versus* the number of CH_2 groups in **8a–f**

Characterization of polyimides 8a–f

When d.s.c. measurements were conducted at a heating and cooling rate of 20°C min^{-1}, two strong endotherms were detectable in the heating curves (*Figure 6*). The intensity of both endotherms suggests that they represent a melting process and the isotropization of a smectic LC phase. The corresponding two exotherms are observable in the cooling traces, with the low-temperature exotherm showing a significant undercooling effect, typical for a crystallization process, and the high-temperature exotherm indicating the formation of an LC phase from the isotropic melt. This interpretation was confirmed by optical microscopy. The melting temperatures (T_m) and isotropization temperatures (T_i) plotted against the number of methylene groups display a weak odd–even effect as illustrated in *Figure 7*. Even more pronounced odd–even effects of T_m were reported for three classes of

poly(ester–imide)s with alkane spacers in the main chain[10,11,28–30].

Because the LC phases were broader upon cooling, the textures were easier to characterize during the cooling cycle. All members of the series **8a–f** exhibited the same textures. During the first cooling cycle a somewhat imperfect 'fan-shaped' texture was observed (*Figure 8*), which may be formed by smectic A or smectic C phases.

Figure 8 Texture observed at 390°C for the first cooling of **8f** from the isotropic melt

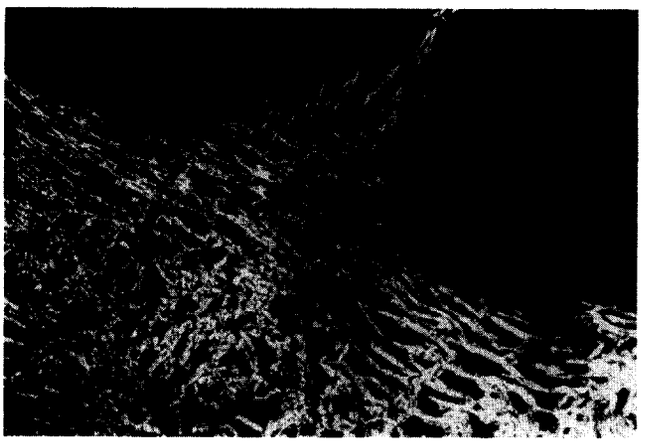

Figure 9 Texture observed at 385°C for the second cooling of **8f** from the isotropic melt

However, the second cooling cycle yielded a 'batonet' texture which is characteristic for a smectic A phase (*Figure 9*). The lengthy birefringent particles 'smear out' when exposed to slight shear forces and relax immediately when the shearing is stopped. This behaviour clearly proves that a mobile smectic melt is formed, and the most mobile smectic phase is the smectic A phase.

The existence of a smectic melt is also evident from X-ray measurements conducted with synchrotron radiation at a heating rate of 20°C min^{-1}. A sharp middle-angle reflection (MAR) is detectable above the melting point (*Figures 10* and *11*). This MAR corresponds to a sharp MAR observable for the solid state, but their positions are not exactly identical (*Figure 11*). In other words, the dimensions of the layer structures are somewhat different for the molten and the solid states. The longer distances (*d* spacings) calculated from the MAR of the smectic melt correspond well to values calculated for linear repeating units with upright mesogens and spacers adopting an all-*gauche* conformation (*Table 5* and *Figure 12*). A predominance of *gauche* conformations and partial coiling of the spacers is a reasonable assumption considering the high temperatures under investigation.

Furthermore, a ^{13}C n.m.r. cross-polarization/magic-angle spinning (CP/MAS) spectrum of **8f** was measured at 25°C (*Figure 13*). It exhibits a broad signal at ~30.5 ppm which suggests a predominance of *gauche* conformations and a rapid exchange with a few *trans* conformations even at room temperature. The sharp

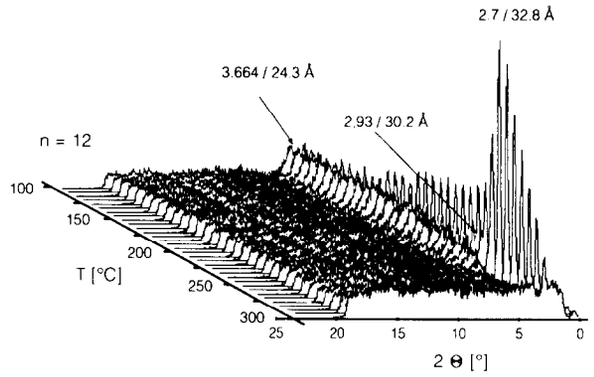

Figure 10 Synchrotron radiation measurements of the middle-angle reflections of polyimide **8f** at a heating rate of 20°C min^{-1}

Table 5 Middle angle reflections (MARs), experimental layer distances and calculated layer distances for polyimides **8a–f**

Polymer	MAR (2θ) at 25°C (°)	*d* spacing[a] (Å)	MAR (2θ) melt (°)	*d* spacing[b] (Å)	*d* spacing[c] all-*gauche* (Å)	*d* spacing[d] all-*trans* (Å)
8a	3.7	19.0±0.3	–	–	25.1	28.8
8b	3.9	19.5±0.3	–	–	26.9	31.1
8c	4.0	20.4±0.3	3.12	28.3±0.3	28.6	33.6
8d	4.3	21.1±0.3	3.07	28.8±0.3	30.3	34.2
8e	4.5	22.9±0.3	2.98	29.7±0.3	32.0	36.2
8f	4.7	23.9±0.3	2.70	32.8±0.3	33.7	37.5

[a] Calculated from the MAR measurement at 25°C
[b] Calculated from the MAR determined from the smectic melt
[c] Calculated for linear repeating units with upright mesogens and all-*gauche* conformation of the spacers
[d] Calculated for linear repeating units with upright mesogens and all-*trans* conformation of the spacers

signal at around 33 ppm typical for alkyl chains with all-*trans* conformation in ordered paraffin domains is clearly not present. In other words, textures, X-ray and ^{13}C n.m.r. CP/MAS measurements agree in that polyimides **8a–f** form a smectic A phase with somewhat coiled, highly mobile spacers. Several poly(ester–imide)s show the same tendency[29–31].

The WAXD patterns and the chain packing of the solid polyimides **8a–f** are more difficult to interpret than those

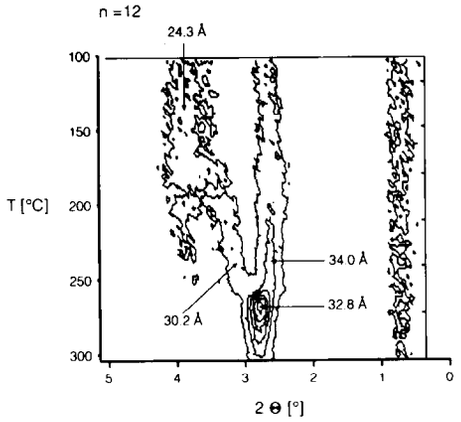

Figure 11 Contour map of the middle-angle reflections of polyimide **8f** measured with synchrotron radiation at a heating rate of 20°C min^{-1} (see *Figure 10*)

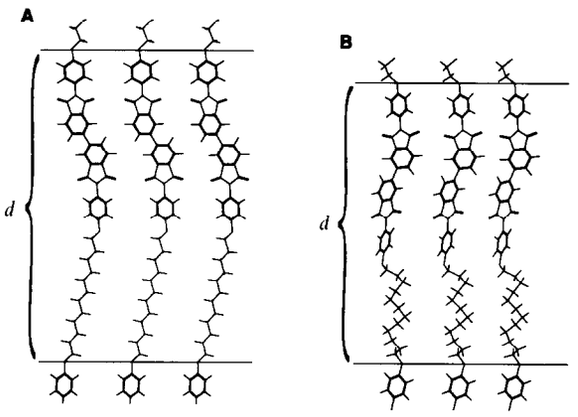

Figure 12 Scheme of layer structures with upright mesogens and all-*trans* (A) or all-*gauche* (B) conformation of the spacers, as obtained by computer modelling with the force-field program PCFF 91/Insight II V 2.2.0/Discover V 2.8.0 from Biosym

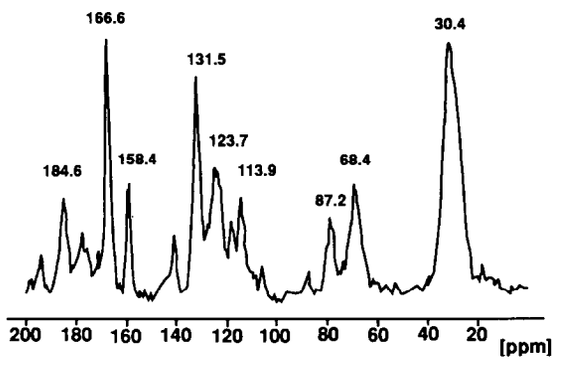

Figure 13 ^{13}C n.m.r. CP/MAS spectrum at 75.4 MHz of polyimide **8f**

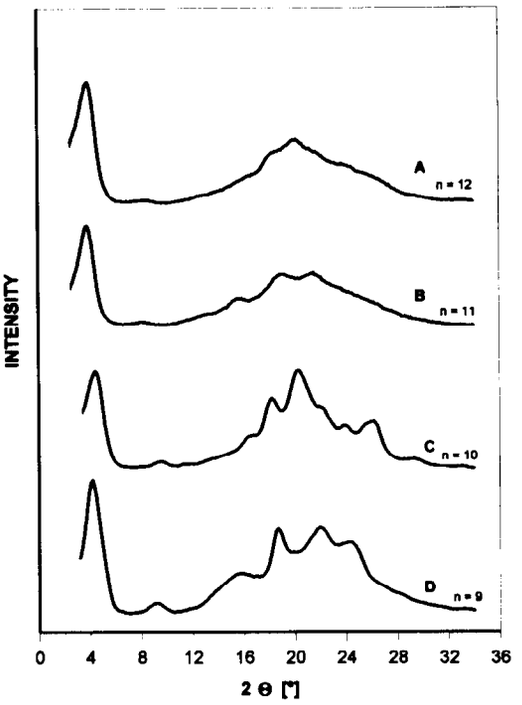

Figure 14 WAXD powder patterns polyimides **8f** (A), **8e** (B), **8d** (C) and **8c** (D)

of the molten state, and only some preliminary results will be reported in this work. All samples precipitated into methanol and dried at 120°C display two MARs (*Figures 10* and *11*): a sharp reflection in the range $2\theta = 28–33°$ and broader reflection in the range of $2\theta = 19–24°$. This second reflection, which can be measured even in the presence of air (*Figure 14*), is not a higher order of the sharper reflection. Furthermore, it disappears in the molten state (*Figures 10* and *11*) and does not reappear upon cooling. When treated as a first-order reflection, the broad MAR corresponds to atomic distances of the order of 19–24 Å (*Table 5*) which are difficult to interpret.

The WAXD powder patterns also display several reflections in the range $2\theta = 15–30°$ which indicate that **8a–f** do not adopt a hexagonal chain packing in the solid state. The gradual change of these patterns (*Figure 14*) with the lengths of the spacers fits in with a change from three-dimensional crystal lattices (e.g. orthorhombic or monoclinic) to two-dimensional crystals, i.e. layer structures of the smectic E or H type. A more detailed study of the chain packing in the solid state is in progress and will be published in due course.

CONCLUSION

The results of this work indicate that the diphenyltetracarboxylic imide unit is a poor mesogen. Only in combination with *para*-substituted phenylene groups may LC phases be formed. The coplanarity of all the rings seems to play an important role in stabilization of the mesophase. The contrast between polar imide groups and non-polar alkane chains favours the formation of layer structures in the solid and in liquid states. For the first time, thermotropic polyimides free of ester groups were obtained.

REFERENCES

1 Cassidy, P. E. 'Thermally Stable Polymers', Marcel Dekker Inc., New York, 1982, Ch. 5
2 Mittal, K. L. (Ed.) 'Polyimides', Plenum Press, New York, 1982, Vol. 1
3 Elias, H.-G. and Vohwinkel, F. 'Neuer Polymere Werkstoffe', 2nd edn, Hanser Verlag, München, 1983, Ch. 11, p. 257
4 Verbicky, W. Jr in 'Encyclopedia of Polymer Science and Engineering' (Eds M. Bikales, H. F. Mark, G. C. Overberger and G. Menges), 2nd edn, Wiley & Sons, New York, 1988, Vol. 12, p. 363
5 Sillion, B. in 'Comprehensive Polymer Science' (Eds G. Allen and J. C. Bevington), Pergamon Press, Oxford, 1989, Vol. 5, Ch. 30
6 Alam, S., Kandpal, L. D. and Varma, I. K. *J. Macromol. Sci., Res. Macromol. Chem. Phys.* 1993, **33**, 291
7 De Abajo, J. in 'Handbook of Polymer Synthesis' (Ed. H. R. Kricheldorf), Marcel Dekker Inc., New York, 1992, Ch. 15
8 Sroog, C. E. *Prog. Polym. Sci.* 1991, **16**, 561
9 Irwin, R. I. *U.S. Pat. 4 176 223*, E. I. Du Pont de Nemours Co., 1979
10 Kricheldorf, H. R. and Pakull, R. *Polymer* 1987, **28**, 1772
11 Kricheldorf, H. R. and Pakull, R. *Macromolecules* 1988, **21**, 551
12 Kricheldorf, H. R. and Pakull, R. *Macromolecules* 1988, **21**, 1929
13 Kricheldorf, H. R. and Pakull, R. *New Polym. Mater.* 1989, **3**, 165
14 Kricheldorf, H. R., Pakull, R. and Buchner, S. *J. Polym. Sci. Part A, Polym. Chem.* 1989, **27**, 431
15 Kricheldorf, H. R. and Hüner, R. *Makromol. Chem., Rapid Commun.* 1990, **11**, 211
16 De Abajo, J., De La Campa, J., Kricheldorf, H. R. and Schwarz, G. *Makromol. Chem.* 1990, **191**, 537
17 Kricheldorf, H. R., Domschke, A. and Schwarz, G. *Macromolecules* 1991, **24**, 1011
18 Kricheldorf, H. R., Schwarz, G., Domschke, A. and Linzer, V. *Macromolecules* 1993, **26**, 5161
19 Mustafa, I. F., Al-Dujaili, A. H. and Alto, A. T. *Acta Polym.* 1990, **41**, 310
20 Sato, M., Hirata, T. and Mukaida, V. *Makromol. Chem.* 1992, **193**, 1729
21 Griffin, A. C., Britt, T. R., Hung, R. S. L. and Steele, M. L. *Mol. Cryst. Liq. Cryst.* 1984, **105**, 305
22 Hirata, T., Sato, M. and Mukaida, K. *Makromol. Chem.* 1993, **194**, 2861
23 Kricheldorf, H. R., Linzer, V. and Bruhn, J. M. S. *Pure Appl. Chem.* 1994, **131**, 1315
24 Kricheldorf, H. R., Linzer, V., De Abajo, J., De la Campa, J. and Bruhn, J. M. S. *Pure Appl. Chem.* in press
25 Onsager, L. A. *Ann. N.Y. Acad. Sci.* 1949, **51**, 627
26 Flory, P. J. *Proc. R. Soc. London* 1956, **A234**, 73
27 Flory, P. J. and Ronca, G. *Mol. Cryst. Liq. Cryst.* 1979, **54**, 311
28 Kricheldorf, H. R., Schwarz, G., De Abajo, J. and De La Campa, J. *Polymer* 1991, **32**, 941
29 Kricheldorf, H. R., Schwarz, G., De Abajo, J. and De la Campa, J. *Macromolecules* 1994, **27**, 2540
30 Pardey, R., Shen, D., Cabori, P. A., Harris, F. W., Cheng, S. Z. D., Aducci, J., Facinelli, J. V. and Lenz, R. W. *Macromolecules* 1993, **26**, 3687
31 De Abajo, J., de la Campa, J., Kricheldorf, H. R. and Schwarz, G. *Polymer* 1994, **35**, 5577